

Received April 02, 2024; accepted July 26, 2024; Date of publication August 06, 2024.

The review of this paper was arranged by Associate Editor Edivan L. C. da Silva and Editor-in-Chief Heverton A. Pereira.

Digital Object Identifier <http://doi.org/10.18618/REP.2005.2.017021>

# An Analysis of the Limitations of Power Smoothing Metrics and Future Perspectives for Their Evolution in the Context of BESS-Based Systems

Ricardo M. de Souza<sup>1</sup>, Felipe J. P. Ferreira<sup>1</sup>, Antonio S. Neto<sup>2</sup>,  
Rafael C. Neto<sup>1</sup>, Francisco A. S. Neves<sup>1</sup>, José F. C. Castro<sup>1</sup>

<sup>1</sup>Federal University of Pernambuco, Department of Electrical Engineering, Recife – Pernambuco, Brazil.<sup>2</sup>Universidade de Pernambuco, Escola Politécnica de Pernambuco, Recife – Pernambuco, Brazil.

e-mail: ricardo.mourasouza@ufpe.br, felipe.jpferreira@ufpe.br, asneto01@poli.br, rafael.cavalcantineto@ufpe.br, francisco.neves@ufpe.br, filho.castro@ufpe.br.

**ABSTRACT** The growing presence of power ramps, typically caused by the intermittency of renewable energy sources (RESs), may ultimately threaten the stability and reliability of the power grid. In the context of power smoothing algorithms such as Moving Average, Ramp Rate and First-Order Low-Pass Filter have been widely used in reference generation for Energy Storage Systems (ESSs). In this scenario, this paper analyzes typical metrics used for evaluating power smoothing techniques and comments on their limitations. Validation of this analysis is conducted using PV generation data sourced from the National Renewable Energy Laboratory (NREL). The results highlight the need to develop new metrics for a fairer comparison. Finally, this work also sets a concrete path for the evolution of said metrics.

**KEYWORDS** Battery energy storage system, power fluctuation, power smoothing, ramp rate.

## I. INTRODUCTION

The potential impacts of climate change on various aspects of human activities are profound, as they can lead to infrastructure damage, disrupt water and food availability for populations, and trigger mass displacements. This situation becomes particularly alarming when considering that, despite historical emissions being concentrated in developed countries, the most vulnerable nations are those with lower per capita emissions and fewer resources to address the issue [1].

The described scenario invites for global actions with the aim of minimizing climate change. In this context, the most recent report released by the Intergovernmental Panel on Climate Change (IPCC) lists options for climate change mitigation, categorizing them according to their potential contributions to short-term emission reductions. These alternatives include measures such as energy efficiency, urban planning, development and application of new materials, and the transition to renewable energy sources (RES). The latter, focusing on wind and photovoltaic (PV) generation, is highlighted in the report as having the greatest potential for short-term emission reduction [1].

The urgency of reducing greenhouse gas emissions is compounded by the recent rise in the competitiveness of technologies linked to renewable sources, as well as by advancements in legislation. This, combined with the immense potential yet to be fully explored, has created the perfect environment for the rapid growth of renewable sources. In Brazil, this growth is evidenced by the installed capacity of plants under the centralized and scheduled dispatch control

of the National Electric System Operator (ONS in its Portuguese acronym), as shown in Fig. 1.

However, despite their advantages, these renewable alternatives also have some negative characteristics. For instance, researchers often discuss concerns such as frequency deviations, voltage flickers, and the need for larger power reserves, all originating from the unpredictable nature of power fluctuations [2]. To address some of these issues, system operators have reviewed and updated their requirements and standards, also known as grid codes, for the integration of RES into power grids. In doing so, they ensure that RES can be incorporated without compromising the stability and reliability of the electrical system [3].

A grid code is a set of technical specifications and requirements that Transmission System Operators define to regulate the operation, connection, and integration of power plants and other electricity-generating facilities into the electrical

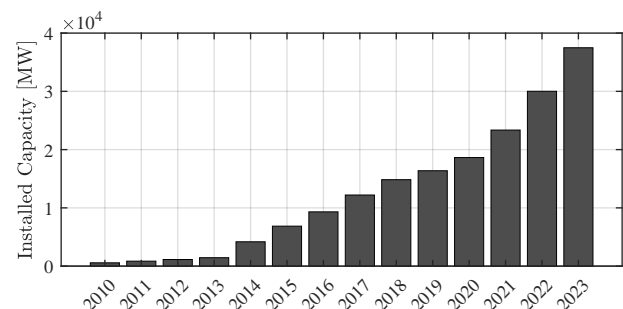


FIGURE 1. Installed capacity of wind and PV power plants under the centralized and scheduled dispatch control of the ONS (Brazil).

grids. These requirements often involve imposing a limitation to upward and downward ramp rates in PV and wind power plants to mitigate the impact of power fluctuations due to RES generation [4]. Some examples of such limitations are listed below:

- In China, national standards dictate that the maximum ramp rate should be less than 10% of the installed capacity per minute, with additional specifications based on voltage levels outlined by the State Grid Corporation of China (SGCC) [5] [6];
- The German grid code stipulates that PV plants must increase their active power post-reconnection at a rate not exceeding 10% of the rated power per minute, for installations exceeding 1 MVA [7]; and
- The European Network of Transmission System Operators for Electricity (ENTSO-E) allows regional Transmission System Operators to set specific ramp rate limits as needed [8], not requiring specific upward or downward rap rates.

These regulations aim to ensure grid stability by controlling the rate at which active power can increase or decrease, thereby smoothing out potential fluctuations caused by the intermittent nature of solar energy [4]. Table 1 summarizes the regulation of upward and downward ramp rates in various countries [9].

Both upward and downward ramp rates limits can be achieved by regulating the power variability of the RES generation. With this in mind, several solutions have been proposed in the literature to address the challenges related with power variability in RES. Conventional methods are predominantly centered solely on control strategies, such as pitch angle control, inertia control and DC link voltage control [10]. However, these approaches frequently result in power dissipation due to the absence of energy storage capabilities. Other research focus on employing Energy Storage Systems (ESSs) to implement smoothing approaches, utilizing technologies such as flywheels, supercapacitors, superconducting magnets, battery energy storage systems (BESSs), and hybrid configurations [11].

In recent years, there has been a notable rise in the competitiveness of BESSs, largely driven by their expanded utilization in the electronics and automotive industries. Electric vehicles (EVs) are especially significant in this context

**TABLE 1. Maximum active power ramp rate requirements defined in the grid codes of various countries.**

Country	System Operator	Upward Ramp Rate	Downward Ramp Rate
Germany	E.ON	10%/min	Not required
Ireland	EIRGRID	30 MW/min	Not required
Mexico	CENACE	2~5%/min	1~5%/min
Puerto Rico	PREPA	10%/min	10%/min
European Standards	ENTSO-E	Not required	Not required

since their batteries can be utilized for power smoothing, thus potentially eliminating the need to install BESSs in certain contexts. An example of EVs being employed in this manner can be found in [12]. Within the realm of power fluctuation management, various BESS-based strategies, also referred to as power smoothing systems, have emerged in the literature.

The effectiveness of these systems, particularly in their utilization for power smoothing purpose, strongly depends on the algorithm employed for reference generation, which, according to [13], can be classified into the following families: moving average and exponential smoothing-based approaches; filter-based methods; and ramp rate control algorithm-based techniques. However, the performances of these methods are often evaluated through visual analysis or employing metrics that may result in unjustified comparisons or flawed conclusions [11] [2].

In this scenario, the primary objective of this paper is to examine the most common metrics used to evaluate the effectiveness of power smoothing schemes. To accomplish this, three distinct reference generation algorithms are employed to smooth the power output of two PV power plants, whose data was generated by NREL (National Renewable Energy Laboratory). To the best of the authors' knowledge, the present paper has the following original contributions:

- A performance comparison among three widely used power smoothing strategies in the literature, one from each classification family;
- An evaluation of limitations and a qualitative comparison of the main metrics used in the literature to compare the performance of power smoothing strategies; and
- A guideline for developing new improved metrics, with statistical significance, for power smoothing applications.

It is important to indicate that the present work is a post-conference version of [14]. Compared to the paper published at the conference, this article broadens the number of compared power smoothing strategies and deepens the evaluation of metric limitations. Additionally, this paper adds on to the original article by including a qualitative comparison and guidelines for developing new metrics. Since the present article is focused on evaluating the limitations of power smoothing metrics, assessing the requirements for storage systems sizing for different algorithms is not within its scope.

The paper is structured as follows. Section II presents the operating principles of power smoothing systems based on BESS. In Section III, three traditional algorithms commonly used for reference signal generation in power smoothing systems are presented. Section IV is focused on the standard metrics used in the literature to evaluate the aforementioned algorithms. Subsequently, Section V provides a qualitative comparison and outlines the limitations of the evaluated metrics, while also proposing methodologies for developing new metrics. Lastly, the conclusions are presented in Section VI.

## II. POWER SMOOTHING SYSTEMS BASED ON BATTERY ENERGY STORAGE SYSTEMS

As described in Section I, the intermittent nature of RESs introduces undesirable power fluctuations on the electric grid to which they are connected. Traditional methods to minimize this problem rely on operating the interface converters away from the maximum power point (MPP) of the RES, resulting in the loss of some generated energy. Examples of power smoothing strategies that do not rely on the use of ESS can be found in [15]–[17]. However, there are several alternatives capable of keeping the system operating at its maximum generation capacity while simultaneously achieving the power smoothing objective.

In this context, ESSs serve as a vital solution for mitigating power fluctuations originating from renewable generation, both in the short and long term, ensuring their operation at the MPP. In addition to mitigating immediate fluctuations, ESSs allow for maintaining the operational efficiency of the renewable source by continuously optimizing its operating point [10]. This approach significantly enhances the stability and reliability of the energy system, facilitating a more effective and sustainable integration of RESs into the energy matrix. An example of a system incorporating PV generation and BESS is illustrated in Fig. 2.

As shown in Fig. 2, a power smoothing system based on BESS consists of an energy storage system and a static converter connecting it to the point of common coupling (PCC). This setup is responsible for injecting/absorbing power at the PCC, ensuring that the power delivered to the grid is smoothed out in accordance with regulatory requirements associated with power fluctuations. This setup includes a reference generator that calculates the reference active power to be injected by the BESS at the PCC, denoted as  $P_{BESS}^*(t)$ . Once this reference active power is determined, the static converter, acting as an interface for the BESS, is controlled to inject/absorb the power  $P_{BESS}(t)$  by defining the duty cycles of its semiconductor switches, represented here as  $d(t)$ . It is important to note that the BESS cannot inject power into the grid if it does not have sufficient

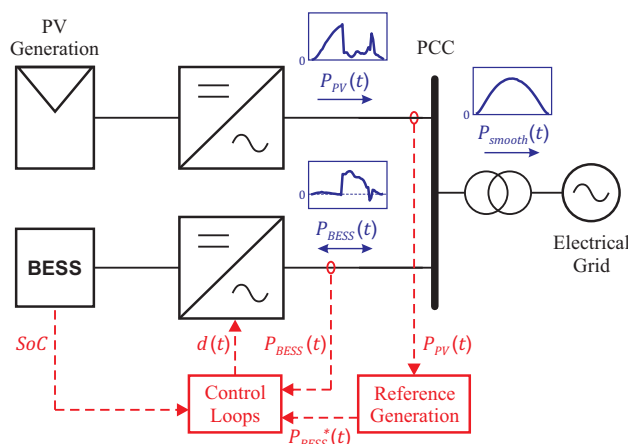


FIGURE 2. Example of power smoothing system based on BESS.

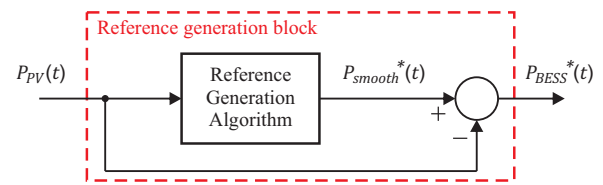


FIGURE 3. Simplified block diagram of a conventional power smoothing control scheme based on the use of BESS.

charge, thus requiring the evaluation of its state of charge (SoC). Although voltage and current measurements are not shown in Fig. 2, it must be highlighted that this information is essential for implementing the converter’s control loops.

The reference generator block is responsible for defining the power to be injected/absorbed by the BESS in order to implement power smoothing. It typically operates as shown in Fig. 3, i. e., it involves measuring the active power generated by the renewable energy source,  $P_{PV}(t)$ , and applying it on a reference generation algorithm, which is responsible for smoothing out the active power  $P_{PV}(t)$  to obtain  $P_{smooth}^*(t)$ . Finally, to determine the power reference for the power smoothing system, one must calculate:

$$P_{BESS}^*(t) = P_{smooth}^*(t) - P_{PV}(t). \quad (1)$$

As a consequence, the reference generation algorithm plays a significant role in this system. However, there is a wide variety of possible reference generation algorithms for this application, each generating a different power profile to be injected at the PCC. In order to observe such variety, Fig. 4 presents the three families of reference generation algorithms that are commonly used for power smoothing applications. In this context, it is important to better understand the families of reference generation algorithms available in the literature and the most commonly used metrics for analyzing and comparing these algorithms.

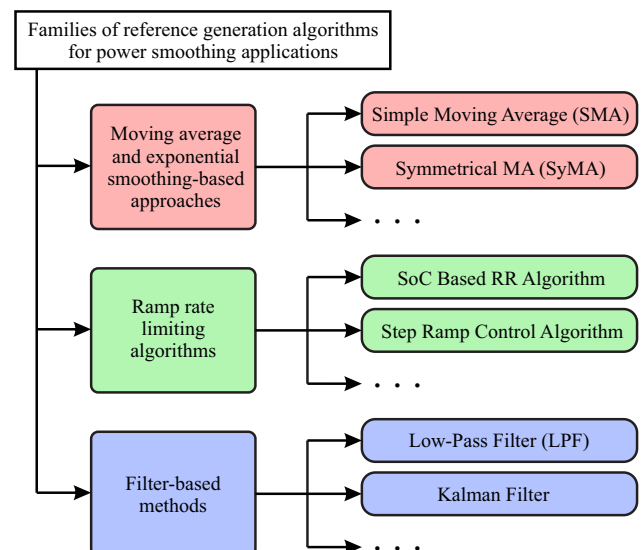


FIGURE 4. Families of reference generation algorithms for power smoothing applications.

### III. REFERENCE GENERATION ALGORITHMS FOR POWER SMOOTHING APPLICATIONS

In the context of power smoothing, the primary aim is to reduce the impact of fluctuations in power output. This is typically achieved by minimizing the rate of change of power over time, known as the ramp rate (distinct from the set of techniques referred to as "Ramp Rate" and denoted in uppercase letters). While there might be slight variations in its definition, the ramp rate is commonly employed in various grid regulations to constrain allowable variations [2] [3]. In this work, the ramp rate is defined as the average rate of power change.

In order to align the discussion with the study of increment statistics – and considering that the rate ( $\Delta P/\Delta t$ ) and the variation ( $\Delta P$ ) only differ by a constant multiplier – this work does not consider the rate of change per se, but rather the differences in power between consecutive measurements, spaced apart by a time interval  $\Delta t$ . The selection of  $\Delta t$  determines the frequency of analysis and subsequently influences the nature of the phenomenon under scrutiny. In the following sections, consider a collection of power measurements denoted as  $P = \{P_1, P_2, \dots, P_N\}$ , taken at intervals of  $\Delta t$ , for which the changes in power are represented by  $\Delta P = P_k - P_{k-1}$ . These increments can be positive or negative, contingent upon the direction of the change.

As briefly introduced in Section I, several power smoothing strategies based on BESS can be found in the literature. These strategies are commonly classified by the algorithm family used in their reference generation block, as illustrated in Fig. 4. According to this classification, the reference generation algorithms can be divided into three distinct categories [13]: (i) moving average and exponential smoothing-based approaches; (ii) ramp rate limiting algorithms; and (iii) filter-based methods.

In the following subsections, a summary of one reference generation algorithm from each of the aforementioned families is presented. These algorithms are used in this paper to analyze the metrics used for evaluating reference generation algorithms in power smoothing systems.

#### A. Simple Moving Average – SMA

The moving average is a statistical method that achieves energy smoothing by computing the average value within a specified rolling window of data [18]. The Simple Moving Average (SMA) is the most common method of applying the moving average to a data sequence, and it consists of calculating the arithmetic average of a window of  $n$  sequential elements from a data set, considering this moving window over time. The mathematical representation of the SMA, for a window of  $n$  elements, adapted from [19], is given by:

$$P_{SMA,k} = \frac{1}{n} \sum_{j=0}^{n-1} P_{k-j}, \quad (2)$$

in which  $n \leq k$ , where  $k$  is an index of the data sequence comprising the sample space, and  $j$  is an auxiliary index used for calculating the moving average. The maximum possible variability ( $\Delta P_{max}$ ) is a fraction of the maximum natural variability ( $\Delta P_{max}^{nat}$ ) of the power plant [20], as in:

$$\Delta P_{max} = \frac{1}{n} \Delta P_{max}^{nat}. \quad (3)$$

#### B. Ramp Rate – RR

The RR method controls power generation variability by restricting the rate at which the power output can change within a specific time period [21]. Therefore, in general, when a large variation in power generation occurs, one can make the rate of growth/decrease in injected/absorbed power from the grid remains constant. In doing so, the energy production becomes limited to the maximum allowable ramp rate ( $\pm\lambda$ ).

Then, the RR method can be represented by:

$$P_{RR,k} = \begin{cases} P_{RR,k-1} + \lambda, & \text{if } \Delta P > \lambda; \\ P_{RR,k-1} - \lambda, & \text{if } \Delta P < -\lambda; \\ P_k, & \text{otherwise;} \end{cases} \quad (4)$$

and its maximum possible variability is given by:

$$\Delta P_{max} = \lambda. \quad (5)$$

#### C. First-Order Low-Pass Filter – LPF

Filters are widely used to attenuate or enhance certain characteristics of signals, such as amplitude, phase or frequency response. Depending on the characteristic, the filter may allow the passage of certain frequency bands of the signals. A typical example is low-pass filters, which retain harmonic content below the cutoff frequency,  $f_c$ , while attenuating signal harmonic components with higher frequencies.

The representation of the first-order low-pass filter (LPF) can be obtained by applying the Laplace transform to a first-order ordinary differential equation with linear coefficient and constant. Thus, the transfer function of the LPF can be represented as:

$$H_{LPF}(s) = \frac{1}{\tau s + 1}, \quad (6)$$

in which  $\tau$  represents the time constant of the first-order LPF in seconds. When discretized using forward Euler method, the first-order LPF can be implemented as follows:

$$P_{LPF,k} = \left(1 - \frac{\Delta t}{\tau}\right) P_{LPF,k-1} + \frac{\Delta t}{\tau} P_{k-1}, \quad (7)$$

where  $\Delta t$  is the sampling period. The maximum possible variability obtained by applying this reference generation strategy is given by:

$$\Delta P_{max} = \frac{\Delta t}{\tau} \Delta P_{max}^{nat}. \quad (8)$$

#### IV. COMMON POWER SMOOTHING METRICS

The choice and evaluation of power smoothing algorithms are inherently interrelated tasks. Power smoothing analysis can be understood as a comparative analysis of power variability before and after the application of the smoothing methods. As it is a complex phenomenon, power variability cannot be analyzed in a one-dimensional manner. To prevent this from happening, power smoothing can be analyzed through the categorization of power variability effect time range, the severity of the variability and/or its probability [2].

As done in [14], the present paper only investigate metrics that are associated with the severity and the probability of the variations. This happens because the time range of the study (and its effects) are predefined by the sampling frequency of the dataset. Additionally, as emphasized in [14], it is essential to recognize that a robust metric should possess the following characteristics:

- The ability to encapsulate the relevant characteristics of the observed phenomena regarding their frequency and/or intensity;
- Applicability to systems with distinct generation sources or systems with multiple generation sources;
- The ability to allow comparison of results from different locations and dimensions; and
- Low sensitivity to variations of the number of samples.

In face of this, the most common power smoothing metrics used in the literature are briefly described below.

##### A. Standard Deviation

One of the most common ways to characterize stochastic phenomena is through the use of probability. Probabilistic percentiles can be employed to evaluate power variability issues, such as the effectiveness of power smoothing methods or the sizing of operational reserves necessary to ensure the proper functioning of the grid. Given this, in a significant part of the literature associated with power smoothing, standard deviation ( $\sigma$ ) ends up being a frequently used metric.

The significance of the standard deviation becomes more relevant only when the dataset follows a Gaussian distribution. When this happens, approximately 68,27% of the samples are contained within one standard deviation from the mean ( $\mu$ ). In the context of power smoothing, the calculation of the standard deviation for evaluating a dataset of power variations ( $\sigma_{\Delta}$ ) can be performed as follows:

$$\sigma_{\Delta} = \sqrt{\frac{1}{N-1} \sum_{j=1}^N (P_j - \mu_{\Delta})^2}, \quad (9)$$

where

$$\mu_{\Delta} = \frac{1}{N} \sum_{j=1}^N P_j. \quad (10)$$

Examples of the use of standard deviation in power smoothing applications can be seen in [20] [22]–[24].

##### B. Maximum Variability

From the perspective of regulatory entities, the intensity of power variations is a common concern. Thus, it important that there exist power smoothing metrics capable of considering the calculation of active power variation rates at the point of connection to the grid. In this context, the maximum variation of power observed between sequential measurements within a predefined interval ( $\Delta P_{max}$ ) is typically used to characterize the effectiveness of power smoothing methods.

When using the  $\Delta P_{max}$  metric, the time interval between measurements (sampling period) is commonly associated with the phenomenon under analysis or imposed by operational constraints. However, regardless of the choice of sampling period, the evaluation window used for this analysis in studies focusing on power smoothing analyses is frequently a daily interval. The employed smoothing method is considered satisfactory when it can keep the value of  $\Delta P_{max}$  below a predefined limit throughout the day (or another evaluation window). Examples of its utilization for this purpose can be observed in [19], [25], [26].

##### C. Visual Analysis

Visual analysis provides alternative means of evaluating power smoothing strategies, distinct from numerical metrics like standard deviation and maximum variability. This approach requires plotting the smoothed power profile generated by the studied power smoothing methods onto the original generation profile graph, enabling a visual assessment of the smoothing characteristics. Typically, it is conducted on a daily basis, similar to the common use of the  $\Delta P_{max}$  metric. However, it's worth noting that if a longer power profile is utilized for visual analysis of a power smoothing method, its effectiveness decreases. Fig. 5 shows an example of visual analysis. Further examples of the of visual analysis application in the literature can be found in [27]–[29].

##### D. Irradiance-based Metrics

There are also metrics focused on measuring variability specifically aimed at photovoltaic generation. In these cases, variability is generally calculated based on the deviation of irradiance from the irradiance generated by the clear sky model. An example can be seen in [30]. However, this type of metric is fundamentally limited as it is based on a characteristic unique to photovoltaic generation, which

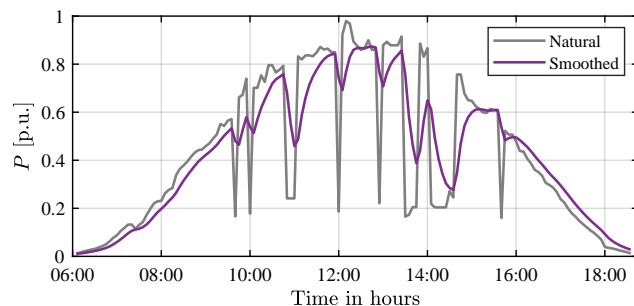


FIGURE 5. Example of Visual Analysis in power smoothing applications.

makes comparisons with other generation sources or between smoothed power curves unfeasible. For this reason, metrics of this nature will not be considered in this work.

**V. ANALYSIS OF THE LIMITATIONS OF COMMONLY USED POWER SMOOTHING METRICS**

In this study, a subgroup of algorithms – representative of the three categories of algorithms used for reference generation in power smoothing applications – is applied to a dataset derived from experimental measurements. Based on the results, the limitations of most commonly used metrics for evaluating power smoothing are examined.

To accomplish this, the experimental data needed to be acquired, preprocessed, and used to validate the power smoothing algorithms. In order to do so, the following six steps were performed:

**1) Acquisition of the Experimental Dataset**

In order to conduct the study presented in this paper, data from two photovoltaic modules located in different sites with distinct climatic characteristics are used. Both datasets were acquired through the project titled "Data for Validating Models for PV Module Performance", coordinated by the National Renewable Energy Laboratory (NREL) [31].

The main advantage of using NREL datasets for this purpose is their public availability, which facilitates any further validation. The two datasets obtained for the current study, with their characteristics summarized in Table 2, correspond to:

- A monocrystalline PV module installed at the Florida Solar Energy Center, in Cocoa (Florida, USA), where a subtropical climate is experienced; and

- A monocrystalline PV module installed at the University of Oregon, in Eugene (Oregon, USA), which is characterized by a marine west coast climate.

**2) Preprocessing the Experimental Database**

In addition to the processing conducted in the original project [32], extra processing steps were necessary due to the dataset’s characteristics.

The time interval between measurements in the dataset is 5 minutes, however, there are gaps in the measurements due to equipment failures, maintenance activities, and potentially shifted intervals. In order to accomplish the objectives of this work, only data points with a difference of 5 minutes were used to populate the processed dataset, ensuring a uniform temporal resolution. Subsequently, the number of points in the dataset for Cocoa and Eugene was reduced to 29.372 and 39.357, respectively.

It is important to disclose that the dataset used for the development of this study does not account for failures that may occur in real-time data acquisition. Thus, it should be recognized that the evaluated algorithms were not assessed regarding their performance in managing such real-time failures.

**3) Evaluation of the Natural Variability**

With the aim of analyzing the efficiency of power smoothing algorithms and, consequently, evaluating commonly used metrics, it is necessary to compare the probability distribution before and after the application of the smoothing methods. With this in mind, using the data processed in Step 2, two diagrams are generated with the per unit variations of power for a 5-minute interval between measurements. These

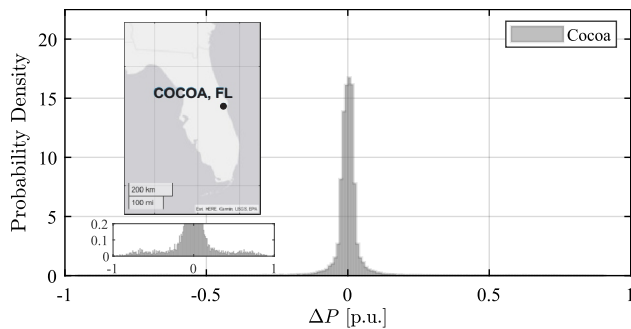


FIGURE 6. Histogram of active power variations normalized for probability density for Cocoa.

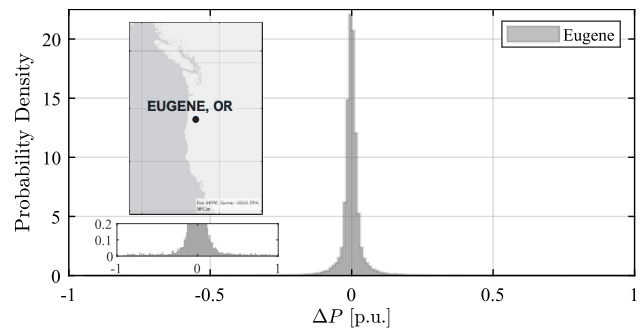


FIGURE 7. Histogram of active power variations normalized for probability density for Eugene.

TABLE 2. Characteristics of the datasets.

Site name	$P_{rated}$ [W]	Approx. location coordinates	Period of measurement	Time between measurements	Number of data points	PV module technology
Cocoa	46.1	28.39 N, 80.75 W	Jan 21, 2011 - Feb 24, 2012	5 min	35,841	Monocrystalline
Eugene	46.1	44.05 N, 123.07 W	Dec 20, 2012 - Jan 19, 2014	5 min	43,174	Monocrystalline

P.S.: The datasets used in this article are publicly available.

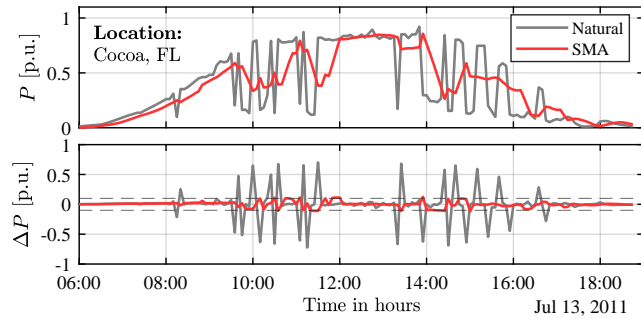


FIGURE 8. Example of daily generation profile before and after smoothing using SMA method. Results for Cocoa on July 13th, 2011.

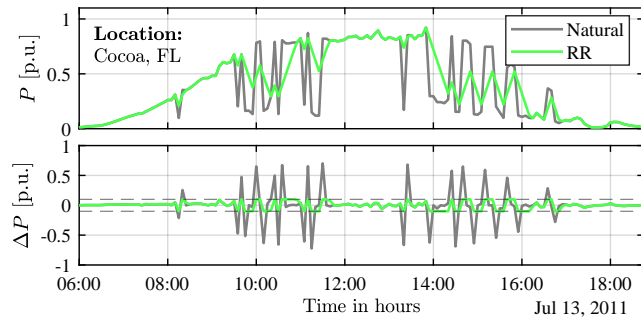


FIGURE 9. Example of daily generation profile before and after smoothing using RR method. Results for Cocoa on July 13th, 2011.

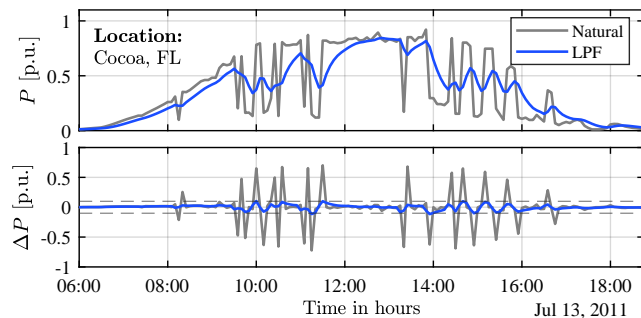


FIGURE 10. Example of daily generation profile before and after smoothing using LPF method. Results for Cocoa on July 13th, 2011.

diagrams depict the natural variability of Cocoa and Eugene and can be observed in Fig. 6 and Fig. 7.

#### 4) Implementation of the Power Smoothing Algorithms

The three power smoothing algorithms evaluated, defined in (2), (4) and (7), were applied to generate power-smoothed profiles from the experimental dataset. These algorithms were implemented using scripts in Matlab and were parameterized to ensure that approximately 99% of the variations after the smoothing remained below the predetermined limit of 0.1 p.u., corresponding to a ramp rate of 0.02 p.u./min. To achieve this:

- For the SMA algorithm, a window of  $n = 6$  samples (30 min) was used for Cocoa, while a window of  $n = 5$  samples (25 min) was used for Eugene;

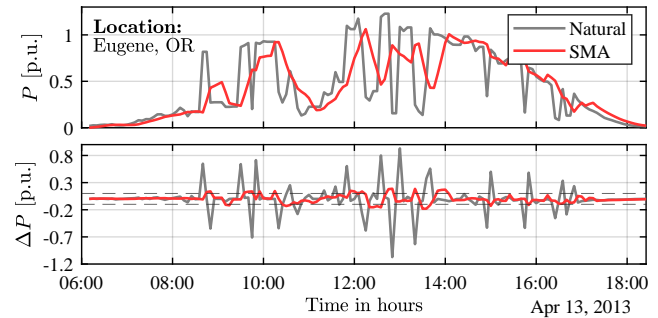


FIGURE 11. Example of daily generation profile before and after smoothing using SMA method. Results for Eugene on April 13th, 2013.

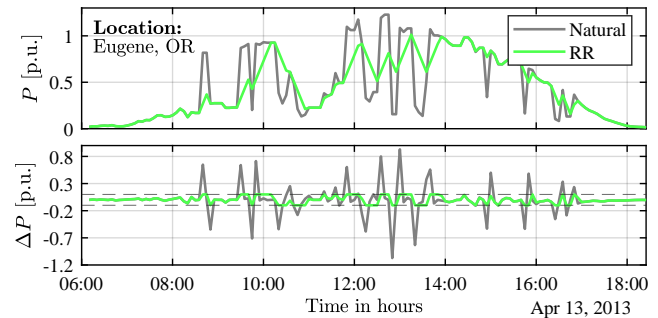


FIGURE 12. Example of daily generation profile before and after smoothing using RR method. Results for Eugene on April 13th, 2013.

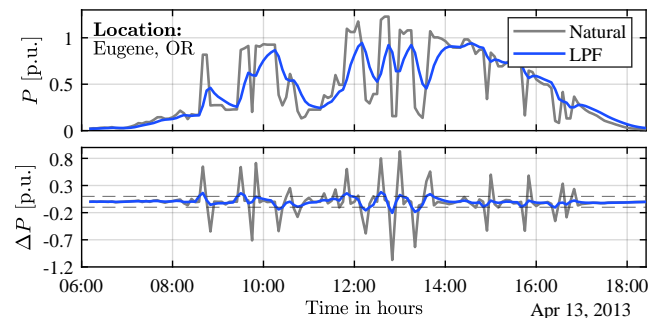


FIGURE 13. Example of daily generation profile before and after smoothing using LPF method. Results for Eugene on April 13th, 2013.

- For the RR algorithm, a ramp rate of  $\lambda = 0.1$  p.u. was applied for both locations; and
- For the LPF algorithm, a filter with a time constant of  $\tau = 1050$  seconds was used for Cocoa, while a time constant of  $\tau = 850$  seconds was applied for Eugene.

#### 5) Results After Power Smoothing

After applying the power smoothing algorithms, a day with severe power variability events was chosen from the dataset for each location for evaluation using visual analysis. Fig. 8, Fig. 9 and Fig. 10 present a daily generation profile before and after applying the evaluated power smoothing techniques algorithms. On the other hand, Fig. 11, Fig. 12 and Fig. 13 present similar results for Eugene. These figures display two graphs: the top one shows the evaluated generation profiles,

while the bottom one presents the power variations before and after the application of smoothing methods. Measurement gaps were filled by substituting missing values with the last recorded measurement to ensure a complete generation profile. However, when considering numerical indicators, only uninterrupted sequences were taken into account. To facilitate visual analysis, the results presented in Figs. 8, 9, and 10 were grouped into a single figure, as shown in Fig. 14.

To evaluate the probability percentiles of the smoothed profiles, new histograms were generated for Cocoa while considering the SMA (Fig. 15), the RR (Fig. 16) and the LPF (Fig. 17) methods. The histograms for Eugene were omitted due to page restriction; however, its numerical indexes were computed for evaluation in Step 6.

## 6) Analysis of the Metrics Limitations

From the results obtained in Step 5, numerical indexes before and after power smoothing were computed, and they are summarized in Table 3. These indexes were calculated considering the entire timeframe available for each location. Based on these results, the limitations of standard deviation, maximum variability and visual analysis are discussed in the following subsections.

### A. Standard Deviation Limitations

After evaluating the results presented in Table 3, it is possible to observe some relevant findings. For the same design requirements, the  $\sigma_{\Delta}$  values differ significantly among the smoothing methods. This occurs even when the analysis is restricted in various ways, as exemplified below:

- **When restricting the analysis to the same location:** The results in Table 3 indicate that, for Cocoa, the  $\sigma_{\Delta}$  values are 0.0229 p.u., 0.0379 p.u. and 0.0231, for SMA, RR and LPF methods, respectively. For Eugene, it is observed that  $\sigma_{\Delta}$  is equal to 0.0216 p.u. for the SMA method, 0.0340 p.u. for the RR method and 0.0217 for the LPF method;
- **When restricting the analysis to the same method:** As presented in Table 3, for Cocoa, the  $\sigma_{\Delta}$  value using the SMA method is 0.0229 p.u., while for the same method in Eugene results in 0.0216 p.u.. On the other hand, when considering the RR method, the  $\sigma_{\Delta}$  value is 0.0379 p.u. for Cocoa and 0.0340 p.u. for Eugene. Finally, when considering the LPF method, the  $\sigma_{\Delta}$  value is 0.0231 for Cocoa and 0.0217 for Eugene.

In summary, when applying the power smoothing algorithms, the  $\sigma_{\Delta}$  values were reduced by 77.8% (SMA), 66.2% (RR) and 77.6% (LPF) in Cocoa, and by 71.2% (SMA), 54.7% (RR) and 71.1% (LPF) in Eugene. It is evident that, although reductions were observed for both locations after smoothing, the value of  $\sigma_{\Delta}$  is not only a function of the methods applied but also of the natural variability of the location. This highlights the limitations of using  $\sigma$  as a metric for directly comparing results between

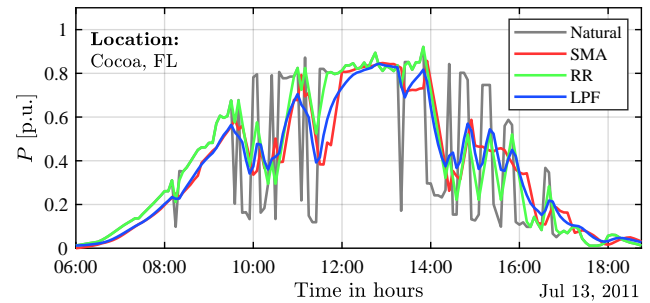


FIGURE 14. Example of daily generation profile before and after smoothing using SMA, RR and LPF methods. Results for Cocoa on July 13th, 2011.

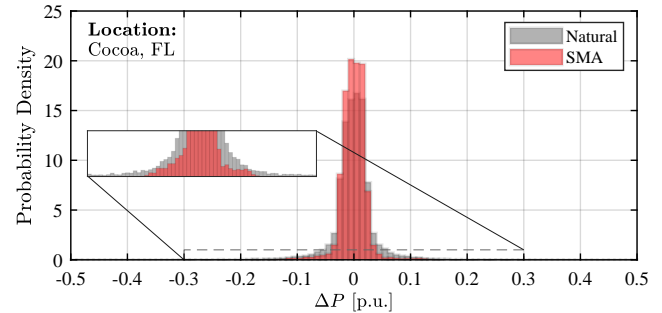


FIGURE 15. Histogram normalized for probability density before and after smoothing using SMA method — Cocoa.

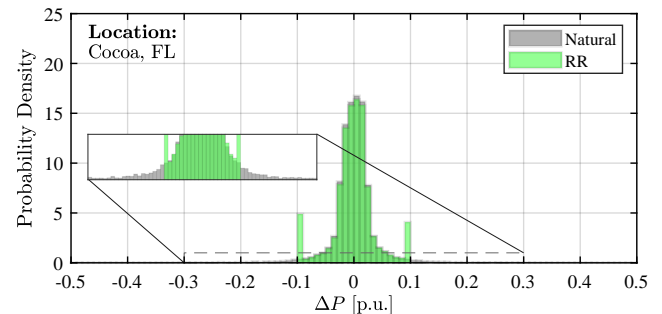


FIGURE 16. Histogram normalized for probability density before and after smoothing using RR method — Cocoa.

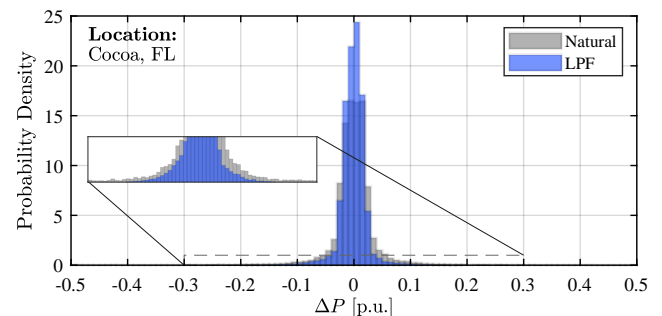


FIGURE 17. Histogram normalized for probability density before and after smoothing using LPF method — Cocoa.

different plants, in addition to its inability, as an indicator, to determine compliance with a given design requirement.

TABLE 3. Numerical indexes before and after power smoothing.

Location	Scenario	$\sigma_{\Delta}$ [p.u.]	$\Delta P_{max}$ [p.u.]	$\sigma_{\Delta,99.73\%}$ [p.u.]	Reduction of $\sigma_{\Delta}^1$
Cocoa	Natural	0.1031	0.953	0.777	–
	SMA	0.0229	0.148	0.125	77.8%
	RR	0.0379	0.100	0.100	66.2%
	LPF	0.0231	0.189	0.137	77.6%
Eugene	Natural	0.0750	0.983	0.736	–
	SMA	0.0216	0.229	0.153	71.2%
	RR	0.0340	0.100	0.100	54.7%
	LPF	0.0217	0.252	0.150	71.1%

TABLE 4. Probability of occurrence of extreme events,  $\mathbb{P}(|\Delta P| \geq x)$ .

Event	Gaussian (%)	Cocoa (%)	Eugene (%)
$ \Delta P  \geq 3\sigma$	0.27	2.53	1.56
$ \Delta P  \geq 5\sigma$	$5.73 \cdot 10^{-5}$	1.53	0.93
$ \Delta P  \geq 7\sigma$	$2.56 \cdot 10^{-10}$	0.51	0.61

TABLE 5. Ratio between the probability of occurrence of the event in the empirical distribution and in an equivalent Gaussian distribution.

Event	Cocoa/Gaussian	Eugene/Gaussian
$ \Delta P  \geq 3\sigma$	9.37	5.78
$ \Delta P  \geq 5\sigma$	26,700	16,230
$ \Delta P  \geq 7\sigma$	1,992,200,000	2,382,800,000

Alternatively, it is worth noting that  $\sigma_{\Delta}$  can be used to evaluate, within the same location, which method requires a larger battery or smaller operational reserves. For the examples studied, the RR method was able to achieve the same design requirements with a higher  $\sigma_{\Delta}$  compared to the SMA and LPF methods. Consequently, this suggests that while the RR method may require a smaller battery, it will demand larger operational reserves.

The values of  $\sigma_{\Delta}$  and  $\sigma_{\Delta,99.73\%}$  demonstrate that the distribution of power variations is not adequately represented by a Gaussian distribution (for which  $\sigma_{\Delta,99.73\%} = 3\sigma$ ), both before and after smoothing. This finding has a significant impact on the analysis of the probability of occurrence of extreme events. For instance, for a  $3\sigma_{\Delta}$  event, the natural occurrence probability for Cocoa and Eugene is, respectively, 9.37 times and 5.78 times higher than that of the equivalent event in a Gaussian distribution, as shown in Table 4 (in absolute terms) and Table 5 (in relative terms).

Since empirical distributions concentrate relatively more probability in their tails, the larger the deviation analyzed, the greater the discrepancy, as can be seen in Table 4 and Table 5. It is thus understood that due to the lack of knowledge regarding which probability distribution adequately represents the natural behavior of the locality, it

is inadequate to evaluate the probability of a given set of variation values based solely on the  $\sigma_{\Delta}$  value.

### B. Maximum Variability Limitations

As discussed in Section IV, the utilization of  $\Delta P_{max}$  typically involves assessing the highest value over a specific 24-hour period. However, it's important to determine the extent to which the maximum values are influenced by sample size and whether the chosen interval of one day holds statistical significance. This concern was addressed through a simulation experiment using experimental samples. This simulation entailed the random selection of one value from the power variations dataset 1,000 times, with the highest value recorded at each iteration. In order to produce multiple  $\Delta P_{max}$  curves (and reduce bias), the simulation was then repeated 5,000 times. The resulting curves for Cocoa and Eugene (obtained by averaging the 5,000 runs) can be seen in Fig. 18 and Fig. 19, respectively. The figures also include  $\sigma_{\Delta}$  at each iteration for reference.

The results depicted in Fig. 18 and Fig. 19 reveal a tendency for  $\Delta P_{max}$  to exhibit a slower convergence towards its true value, i.e., the maximum variability observed across the entire dataset, in contrast to  $\sigma_{\Delta}$ . Considering that each data point in the figure represents a sample, it becomes possible to estimate the anticipated value of  $\Delta P_{max}$  for a given measurement duration by examining the graph at a corresponding iteration count. It's important to highlight that a day's worth of measurements, covering a 12-hour generation period with samples taken every 5 minutes, consists of around 144 samples. Fig. 18 and Fig. 19 demonstrate that both  $\sigma_{\Delta}$  and  $\Delta P_{max}$  display significant variability across the measured sequences over a one-day period. Notably,  $\Delta P_{max}$ 's values continue to exhibit considerable variability even after 1000 iterations, which corresponds to approximately a week's worth of data. This observation prompts the question of how many samples are required for the values of  $\Delta P_{max}$  to converge towards a more reliable measure of the maximum variation present in the dataset.

The potential underestimation of  $\Delta P_{max}$  can have varying implications depending on the algorithm employed. In the case of SMA, underestimating  $\Delta P_{max}$  leads to the selection of a smaller moving window than required, resulting in more frequent occurrences of variations exceeding the permissible limit. In the RR algorithm, the intensity of variations does not impact the method's parameterization. In this case, the consequences of underestimating  $\Delta P_{max}$  manifest as an underestimation of the necessary battery capacity for the algorithm to operate effectively.

### C. Visual Analysis Limitations

As previously noted in discussions regarding  $\Delta P_{max}$  values, visual analysis usually focuses on a single day or a small set of days. Despite the constraints associated with this approach, it conveys important information about smoothing methods. For example, it enables confirmation of the inherent

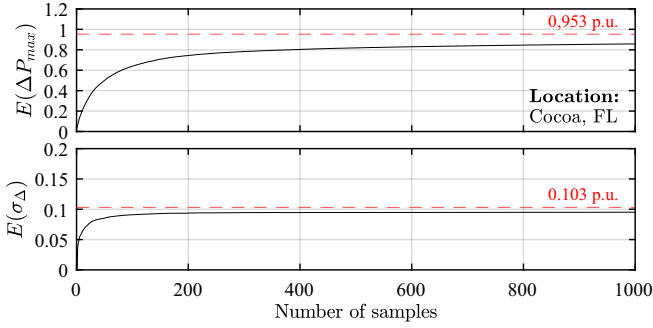


FIGURE 18. Expected values at each iteration ( $\sigma_{\Delta}$  and  $\Delta P_{max}$ ) — Cocoa.

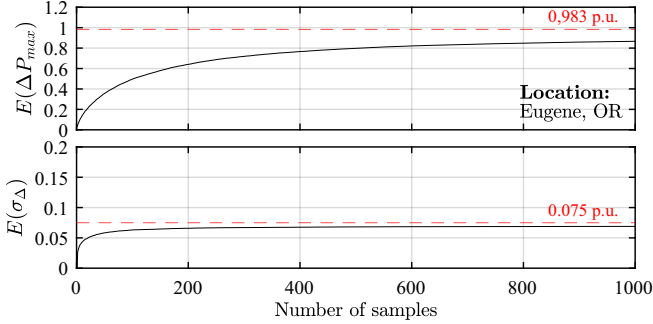


FIGURE 19. Expected values at each iteration ( $\sigma_{\Delta}$  and  $\Delta P_{max}$ ) — Eugene.

delay present in the SMA method. This delay can result in the smoothed curve being either lower or higher than the original curve, depending on the timing, which is a phenomenon not observed with the RR method. It is important to note, however, that relying solely on visual analysis of a single day may not offer an accurate representation of the entire dataset. Moreover, such an approach is susceptible to subjective interpretations by the observer. For example, readers may infer from a comparative examination of Fig. 8 and Fig. 9 (or Fig. 11 and Fig. 12) that the RR method appears to outperform the SMA method, which is not correct, since both methods adequately fulfilled the operational requirements set forth in the study. It could also be inferred that the SMA method yields a higher  $\sigma_{\Delta}$  value than the RR method. However, contrary to expectation, the reality is quite the opposite, which may initially seem counterintuitive.

**VI. QUALITATIVE COMPARISON AND GUIDELINES FOR THE EVOLUTION OF METRICS**

As mentioned in [14] and further discussed in this article, the metrics currently used in the literature for comparing power smoothing techniques have significant limitations. In order to determine guidelines for the evolution of these metrics, a set of criteria should be established. In this context, a metric can be judged by its:

- [I] Ability to rank smoothing methods according to their impact on the need for operating reserves, even if it does not provide relevant information for their sizing;

- [II] Ability to rank smoothing methods according to their impact on the need for operating reserves, while also providing relevant information for their sizing;
- [III] Possibility of being used to compare results from different locations and sizes;
- [IV] Degree of sensitivity to variations caused by the number of samples.

An overview of the performance of the presented metrics concerning these criteria is depicted in Table 6. The limitation of metrics used for probability assessment, namely  $\sigma_{\Delta}$  and  $\sigma_{\Delta,99.73\%}$ , stem from their inability to adequately model the variations of power, which results in poor comparison capabilities. There is also a need for evolution in metrics dedicated to assessing the severity of the variations, such as  $\Delta P_{max}$ , due to its high dependence on the number of samples.

Based on the limitations of the metrics and on the qualitative evaluation presented in Table 6, some suggestions and guidelines for the evolution of these metrics are discussed below:

- The evolution of metrics used for probability assessment demands a better, more rigorous statistical analysis of the phenomena of power variations. This could be achieved through the analysis of the probability density functions (PDFs) and the percentiles of the empirical distribution;
- Still within the domain of probability, another path for evolution can be seen in the characterization of power variability through classical probability distributions, which is a field of study on its own;
- Metrics aimed at evaluating the extent of variations also require evolution. One solution is, through mathematical tools such as Monte Carlo Simulations, determining the number of samples needed for a statistically significant value for  $\Delta P_{max}$ ;

TABLE 6. Qualitative comparison of metrics aimed at analyzing the probability or the severity of power variations.

Criteria \ Metrics	Criteria			
	[I]	[II]	[III]	[IV]
$\sigma_{\Delta}$	✓	✗	✗	low
$\sigma_{\Delta,99.73\%}$	✓	✗	✗	low
$\Delta P_{max}$	✗	✗	✓	high

- ✓ → Fully meets the evaluated criterion;
- ✗ → Partially meets the evaluated criterion;
- ✗ → Does not meet the evaluated criterion.

- Alternatively, a second solution could focus on modeling in order to predict the value of  $\Delta P_{max}$  with fewer samples.

Finally, one may argue that the phenomena observed in this article may be restricted to the sampling interval of the datasets used (5 min). Firstly, it is important to understand that the sampling used is directly associated with the phenomenon under study, and the interval chosen for this work is suitable for, specifically, the study of power smoothing (in order to understand the role of power smoothing in reducing power reserve requirements see [2] and [33]).

Furthermore, it is indeed possible to argue that the results obtained are generalizable to other sampling frequencies, as related literature demonstrates that, within a reasonable range, the sampling rate only affects the intensity of ramps, but not the probability density functions that describe them. In other words, it only affects the value of the parameters, but not the underlying distribution [34] [35]. This means that the obtained results would be valid, even for different sampling periods.

To reassure the reader of the validity of this statement, probability distributions were also obtained for intervals of 10 and 15 min (through downsampling), as can be seen in Figure 20. This figure shows similarities between the three probability distributions, as expected, even when obtaining results with different sampling periods.

## VII. CONCLUSION

In this paper, a brief description of ramp rate requirements on various power grids and the general structure of a power smoothing system based on BESS was presented. Furthermore, typical metrics used to examine power smoothing algorithms were reviewed and compared based on experimental results. The following conclusions can be drawn from the results presented in this work:

- 1) As a metric,  $\sigma_{\Delta}$  is limited in its ability to estimate the probability of variations and should not be used to compare results from different locations;
- 2) The statistical significance of  $\Delta P_{max}$  is highly correlated with the number of samples, making it unsuitable for comparisons in small datasets;

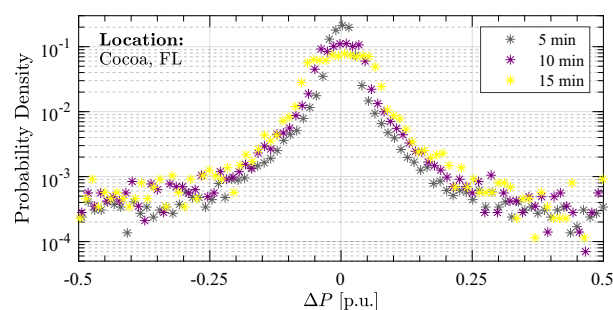


FIGURE 20. Histogram of active power variations normalized for probability density. Data from Cocoa with sampling times of 5, 10, and 15 min.

- 3) Visual analysis is susceptible to subjective interpretations from the observer due to its lack of a numerical index, although it can offer insights into delaying effects; and
- 4) The variations in power cannot be properly characterized by a Gaussian probability distribution.

As a consequence, future works in this field of research should consider the following facts:

- 1) There is a gap in the literature that could be addressed by a more rigorous statistical analysis of power variations in power smoothing settings and their characterization through probability distributions; and
- 2) There is a need in the literature for alternative methods to estimate  $\Delta P_{max}$ , either through anticipation or by determining the number of samples needed for a statistically significant value (which could be achieved with Monte Carlo Simulations).

Collectively, these observations contribute to a deeper understanding of the challenges related to power smoothing algorithm evaluation and, more importantly, offer a roadmap for the evolution of its metrics.

## ACKNOWLEDGMENT

This work was supported in part by the Brazilian Coordination of Superior Level Staff Improvement (CAPES) and in part by EDP group. Besides, the authors would like to thank the EDP group for technical support, through the Research and Development project “E-LOUNGE – A Solution for Electric Vehicle Fleet Charging in Brazil”, with resources from ANEEL’s R&D program under Strategic Call 22 on Electric Mobility.

## VIII. AUTHOR CONTRIBUTIONS

**Ricardo M. de Souza:** Conceptualization, Methodology, Formal analysis, Software, Writing - Original Draft. **Felipe J. P. Ferreira:** Methodology, Software, Validation, Writing - Original Draft. **Antonio S. Neto:** Writing - Review & Editing. **Rafael C. Neto:** Conceptualization, Formal analysis, Validation, Writing - Reviewing and Editing. **Francisco A. S. Neves:** Conceptualization, Writing - Review & Editing. **José F. C. Castro:** Funding acquisition, Writing - Review & Editing.

## PLAGIARISM POLICY

This article was submitted to the similarity system provided by Crossref and powered by iThenticate – Similarity Check.

## REFERENCES

- [1] IPCC, “Summary for Policymakers”, in *Climate Change 2023: Synthesis Report. Contribution of Working Groups I, II and III to the Sixth Assessment Report of the Intergovernmental Panel on Climate Change [Core Writing Team, H. Lee and J. Romero (eds.)]*, pp. 1–34, Geneva, Switzerland, 2023, doi:10.59327/IPCC/AR6-9789291691647.001.
- [2] A. P. Asensio, M. García Plaza, J. López Merino, F. R. Martínez Mendoza, M. Marek Niegowski, P. L. Camuñas García, “Numerical Analysis of Renewable Generation Variability for Energy Storage Smoothing Applications”, in *2021 22nd IEEE International Conference on Industrial Technology (ICIT)*, vol. 1, pp. 446–451, 2021, doi:10.1109/ICIT46573.2021.9453635.

- [3] Y. G. Landera, O. C. Zevallos, R. C. Neto, J. F. d. C. Castro, F. A. S. Neves, "A Review of Grid Connection Requirements for Photovoltaic Power Plants", *Energies*, vol. 16, no. 5, 2023, doi:<https://doi.org/10.3390/en16052093>.
- [4] Q. Zheng, J. Li, X. Ai, J. Wen, J. Fang, "Overview of grid codes for photovoltaic integration", in *2017 IEEE Conference on Energy Internet and Energy System Integration (EI2)*, pp. 1–6, 2017, doi:[10.1109/EI2.2017.8245501](https://doi.org/10.1109/EI2.2017.8245501).
- [5] Standardization Administration of the People's Republic of China, "GB/T 19964-2012 Technical requirements for connecting photovoltaic power station to power system", , 2012.
- [6] State Grid Corporation of China, "Q-GDW 617-2011. Technical requirements for connecting photovoltaic power station to power system", , 2011.
- [7] German VDN e.V. beim VDEW, "Transmission Code 2007: Network and System Rules of the German Transmission System Operators", , 2007.
- [8] European Network of Transmission System Operators for Electricity, "Implementation Guideline for Network Code - Requirements for Grid Connection Applicable to all Generators", , 2013.
- [9] B.-I. Craciun, T. Kerekes, D. Séra, R. Teodorescu, "Overview of recent Grid Codes for PV power integration", in *2012 13th International Conference on Optimization of Electrical and Electronic Equipment (OPTIM)*, pp. 959–965, 2012, doi:[10.1109/OPTIM.2012.6231767](https://doi.org/10.1109/OPTIM.2012.6231767).
- [10] D. Lamsal, V. Sreeram, Y. Mishra, D. Kumar, "Output power smoothing control approaches for wind and photovoltaic generation systems: A review", *Renewable and Sustainable Energy Reviews*, vol. 113, p. 109245, 2019, doi:<https://doi.org/10.1016/j.rser.2019.109245>.
- [11] P. Barra, W. de Carvalho, T. Menezes, R. Fernandes, D. Coury, "A review on wind power smoothing using high-power energy storage systems", *Renewable and Sustainable Energy Reviews*, vol. 137, p. 110455, 2021, doi:<https://doi.org/10.1016/j.rser.2020.110455>.
- [12] M. Raoofat, M. Saad, S. Lefebvre, D. Asber, H. Mehrjedri, L. Lenoir, "Wind power smoothing using demand response of electric vehicles", *International Journal of Electrical Power Energy Systems*, vol. 99, pp. 164–174, 2018, doi:<https://doi.org/10.1016/j.ijepes.2017.12.017>.
- [13] S. Sukumar, M. Marsadek, K. Agileswari, H. Mokhlis, "Ramp-rate control smoothing methods to control output power fluctuations from solar photovoltaic (PV) sources—A review", *Journal of Energy Storage*, vol. 20, pp. 218–229, 2018, doi:<https://doi.org/10.1016/j.est.2018.09.013>.
- [14] R. M. de Souza, F. J. P. Ferreira, A. S. Neto, R. C. Neto, F. A. S. Neves, J. F. C. Castro, "A Comparative Analysis of Power Smoothing Metrics: Unveiling Limitations Through Observational Data", in *2023 IEEE 8th Southern Power Electronics Conference and 17th Brazilian Power Electronics Conference (SPEC/COBEP)*, pp. 1–7, 2023, doi:[10.1109/SPEC56436.2023.10407252](https://doi.org/10.1109/SPEC56436.2023.10407252).
- [15] L. Ran, J. Bumbly, P. Tavner, "Use of turbine inertia for power smoothing of wind turbines with a DFIG", in *2004 11th International Conference on Harmonics and Quality of Power (IEEE Cat. No. 04EX951)*, pp. 106–111, 2004, doi:[10.1109/ICHQP.2004.1409337](https://doi.org/10.1109/ICHQP.2004.1409337).
- [16] T. Senjyu, R. Sakamoto, N. Urasaki, T. Funabashi, H. Fujita, H. Sekine, "Output power leveling of wind turbine Generator for all operating regions by pitch angle control", *IEEE Transactions on Energy Conversion*, vol. 21, no. 2, pp. 467–475, 2006, doi:[10.1109/TEC.2006.874253](https://doi.org/10.1109/TEC.2006.874253).
- [17] A. Uehara, A. Pratap, T. Goya, T. Senjyu, A. Yona, N. Urasaki, T. Funabashi, "A Coordinated Control Method to Smooth Wind Power Fluctuations of a PMSG-Based WECS", *IEEE Transactions on Energy Conversion*, vol. 26, no. 2, pp. 550–558, 2011, doi:[10.1109/TEC.2011.2107912](https://doi.org/10.1109/TEC.2011.2107912).
- [18] *Integration of an Energy Storage System into Wind Farm*, pp. 137–162, Springer London, London, 2009, doi:[https://doi.org/10.1007/978-1-84800-316-3\\_5](https://doi.org/10.1007/978-1-84800-316-3_5).
- [19] R. Kini, D. Raker, T. Stuart, R. Ellingson, M. Heben, R. Khanna, "Mitigation of PV Variability Using Adaptive Moving Average Control", *IEEE Transactions on Sustainable Energy*, vol. 11, no. 4, pp. 2252–2262, 2020, doi:[10.1109/TSTE.2019.2953643](https://doi.org/10.1109/TSTE.2019.2953643).
- [20] A. Puri, "Optimally smoothing output of PV farms", in *2014 IEEE PES General Meeting — Conference Exposition*, pp. 1–5, 2014, doi:[10.1109/PESGM.2014.6939029](https://doi.org/10.1109/PESGM.2014.6939029).
- [21] G. D'Amico, F. Petroni, S. Vergine, "Ramp Rate Limitation of Wind Power: An Overview", *Energies*, vol. 15, no. 16, 2022, doi:<https://doi.org/10.3390/en15165850>.
- [22] T. E. Hoff, R. Perez, "Quantifying PV power Output Variability", *Solar Energy*, vol. 84, no. 10, pp. 1782–1793, 2010, doi:<https://doi.org/10.1016/j.solener.2010.07.003>.
- [23] H. Moaveni, D. K. Click, R. H. Meeker, R. M. Reedy, A. Pappalardo, "Quantifying solar power variability for a large central PV plant and small distributed PV plant", in *2013 IEEE 39th Photovoltaic Specialists Conference (PVSC)*, pp. 0969–0972, 2013, doi:[10.1109/PVSC.2013.6744303](https://doi.org/10.1109/PVSC.2013.6744303).
- [24] A. D. Mills, R. H. Wiser, "Implications of geographic diversity for short-term variability and predictability of solar power", in *2011 IEEE Power and Energy Society General Meeting*, pp. 1–9, 2011, doi:[10.1109/PES.2011.6039888](https://doi.org/10.1109/PES.2011.6039888).
- [25] M. Mitchell, M. Campbell, K. Klement, M. Sedighy, "Power variability analysis of megawatt-scale solar photovoltaic installations", in *2016 IEEE Electrical Power and Energy Conference (EPEC)*, pp. 1–4, 2016, doi:[10.1109/EPEC.2016.7771687](https://doi.org/10.1109/EPEC.2016.7771687).
- [26] A. L. Pinheiro, F. O. Ramos, M. M. B. Neto, R. N. Lima, L. G. S. Bezerra, A. Washington, "A Review and Comparison of Smoothing Methods for Solar Photovoltaic Power Fluctuation Using Battery Energy Storage Systems", in *2021 IEEE PES Innovative Smart Grid Technologies Conference - Latin America (ISGT Latin America)*, pp. 1–5, 2021, doi:[10.1109/ISGTLatinAmerica52371.2021.9543078](https://doi.org/10.1109/ISGTLatinAmerica52371.2021.9543078).
- [27] A. Atif, M. Khalid, "Savitzky–Golay Filtering for Solar Power Smoothing and Ramp Rate Reduction Based on Controlled Battery Energy Storage", *IEEE Access*, vol. 8, pp. 33806–33817, 2020, doi:[10.1109/ACCESS.2020.2973036](https://doi.org/10.1109/ACCESS.2020.2973036).
- [28] S. Koohi-Kamali, N. Rahim, H. Mokhlis, "Smart power management algorithm in microgrid consisting of photovoltaic, diesel, and battery storage plants considering variations in sunlight, temperature, and load", *Energy Conversion and Management*, vol. 84, pp. 562–582, 2014, doi:<https://doi.org/10.1016/j.enconman.2014.04.072>.
- [29] P. L. T. da Silva, P. A. C. Rosas, J. F. C. Castro, D. d. C. Marques, R. R. B. Aquino, G. F. Rissi, R. C. Neto, D. C. P. Barbosa, "Power Smoothing Strategy for Wind Generation Based on Fuzzy Control Strategy with Battery Energy Storage System", *Energies*, vol. 16, no. 16, 2023, doi:<https://doi.org/10.3390/en16166017>.
- [30] S. V. Raygani, R. Sharma, T. K. Saha, "Variability and performance analysis of the PV plant at The University of Queensland", in *2013 Australasian Universities Power Engineering Conference (AUPEC)*, pp. 1–6, 2013, doi:[10.1109/AUPEC.2013.6725342](https://doi.org/10.1109/AUPEC.2013.6725342).
- [31] B. Marion, A. Anderberg, C. Deline, M. Muller, G. Perrin, J. Rodriguez, S. Rummel, T. Silverman, F. Vignola, S. Barkaszi, "Data for Validating Models for PV Module Performance", , 8 2021, doi:<https://doi.org/10.21948/1811521>.
- [32] B. Marion, M. G. Deceglie, T. J. Silverman, "Analysis of measured photovoltaic module performance for Florida, Oregon, and Colorado locations", *Solar Energy*, vol. 110, pp. 736–744, 2014, doi:<https://doi.org/10.1016/j.solener.2014.10.017>.
- [33] H. Holttinen, "Impact of hourly wind power variations on the system operation in the Nordic countries", *Wind Energy*, vol. 8, no. 2, pp. 197–218, 2005, doi:<https://doi.org/10.1002/we.143>.
- [34] M. Anvari, G. Lohmann, M. Wächter, P. Milan, E. Lorenz, D. Heineemann, M. R. R. Tabar, J. Peinke, "Short term fluctuations of wind and solar power systems", *New Journal of Physics*, vol. 18, no. 6, p. 063027, jun 2016, doi:[10.1088/1367-2630/18/6/063027](https://doi.org/10.1088/1367-2630/18/6/063027).
- [35] B. M. Mazumdar, M. Saquib, A. K. Das, "An empirical model for ramp analysis of utility-scale solar PV power", *Solar Energy*, vol. 107, pp. 44–49, 2014, doi:<https://doi.org/10.1016/j.solener.2014.05.027>.

## BIOGRAPHIES

**Ricardo M. de Souza** was born in Recife, Brazil, in 1998. He received his B.Sc. and M.Sc. degrees in electrical engineering from the Federal University of Pernambuco, Recife, Brazil, in 2021 and 2024, respectively. Currently, he is pursuing his Ph.D. degree at the same institution. His research interests include power electronics, renewable energy systems, energy storage systems, and applied probability.

**Felipe J. P. Ferreira** was born in Recife, Brazil, in 2000. He received the B.Sc. degree in control and automation engineering from the Universidade Federal de Pernambuco, Recife, Brazil, in 2024. Currently, he is pursuing his

M.Sc. degree in electrical engineering at the same institution. His researches interests include power electronics, microgrids, energy storage and digital control techniques of static converters.

**Antonio S. Neto** received the B.S. and M.Sc degrees from the Federal University of Pernambuco, Recife, Brazil, in 2003 and 2005, respectively, and since 2022 he has been a doctoral student at PPGEE at UFPE, all in electrical engineering. He started in 2010 as a professor in the Department of Electrical Engineering at the Polytechnic School of Pernambuco-POLI / UPE. He has worked at ONS since October 2005, where he carries out electromagnetic steady-state and transient studies, analyzes of basic projects in the Brazilian Electric System and analyzes of energy quality studies in the integration of wind and solar generation connected to the Interconnected System. His research interests include power electronics, renewable energy systems, storage systems, electromagnetic transients, power quality, and grid-connected converters.

**Rafael C. Neto** was born in Cabo de Santo Agostinho, Brazil, in 1991. He received the B.S. degree in electronic engineering and the M.Sc. and D.Sc. degrees in electrical engineering from the Universidade Federal de Pernambuco, Recife, Brazil, in 2016, 2018, and 2020, respectively. He was a Visiting Scholar with the Universidade Federal de Santa Maria, Brazil, in 2016. Since 2020, he has been with the Department of Electrical

Engineering, Universidade Federal de Pernambuco. His research interests include power electronics, renewable energy systems, and modeling and digital control techniques of static converters.

**Francisco A. S. Neves** received the B.S. and M.Sc. degrees from the Universidade Federal de Pernambuco, Recife, Brazil, in 1984 and 1992, respectively, and the Ph.D. degree from the Universidade Federal de Minas Gerais, Belo Horizonte, Brazil, in 1999, all in electrical engineering. He was a Visiting Scholar with the Georgia Institute of Technology, Atlanta, GA, USA, in 1999, and at the University of Alcalá, Madrid, Spain, from 2008 to 2009. From 1993 to 2023, he was a professor at the Department of Electrical Engineering, Universidade Federal de Pernambuco, Recife, Brazil. His research interests include power electronics, renewable energy systems, power quality, and grid-connected converters.

**José F. C. Castro** holds a Ph.D. from the Pontifical Catholic University of Rio de Janeiro - PUC Rio. He was a Research Analyst at the Energy Research Company - EPE, working on planning the expansion of the Brazilian electrical system. Since 2019, he has been a professor at the Federal University of Pernambuco - UFPE, where he conducts research in the area of microgrid reliability, Distributed Energy Resources, and energy distribution systems.